Drosophila TRIM32 cooperates with glycolytic enzymes to promote cell growth

Simran Bawa, Dr. Erika Geisbrecht
Department of Biochemistry and Molecular Biophysics
Kansas State University

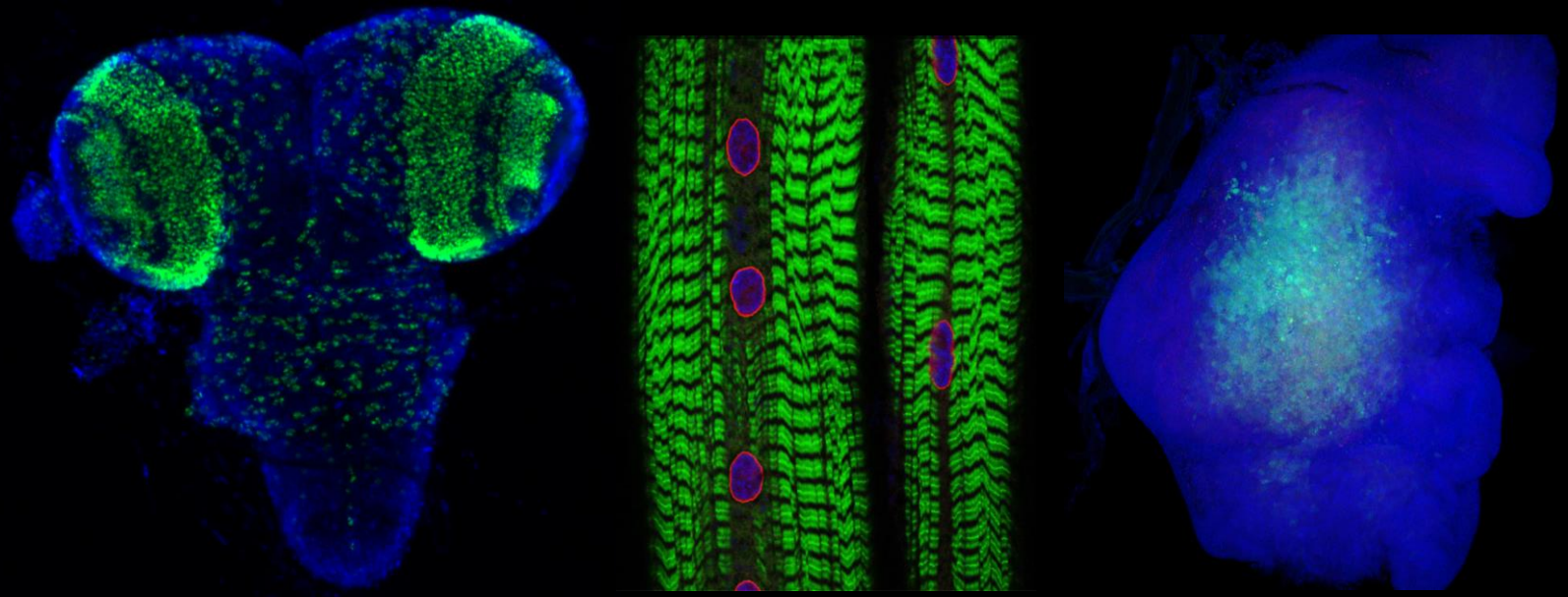

Abstract

Simranjot Bawa1, David S Brooks1, Kathryn E Neville2, Marla Tipping2, Md Abdul Sagar3, Joseph A Kollhoff1, Geetanjali Chawla4,5, Brian V Geisbrecht1, Jason M Tennessen5, Kevin W Eliceiri3, Erika R Geisbrecht1*

Cell growth and/or proliferation may require the reprogramming of metabolic pathways, whereby a switch from oxidative to glycolytic metabolism diverts glycolytic intermediates towards anabolic pathways. Herein, we identify a novel role for TRIM32 in the maintenance of glycolytic flux mediated by biochemical interactions with the glycolytic enzymes Aldolase and Phosphoglycerate mutase. Loss of Drosophila TRIM32, encoded by thin (tn), shows reduced levels of glycolytic intermediates and amino acids. This altered metabolic profile correlates with a reduction in the size of glycolytic larval muscle and brain tissue. Consistent with a role for metabolic intermediates in glycolysis-driven biomass production, dietary amino acid supplementation in tn mutants improves muscle mass. Remarkably, TRIM32 is also required for ectopic growth - loss of TRIM32 in a wing disc-associated tumor model reduces glycolytic metabolism and restricts growth. Overall, our results reveal a novel role for TRIM32 for controlling glycolysis in the context of both normal development and tumor growth.

Figure 1. The NHL region of *Drosophila* TRIM32 is structurally conserved.

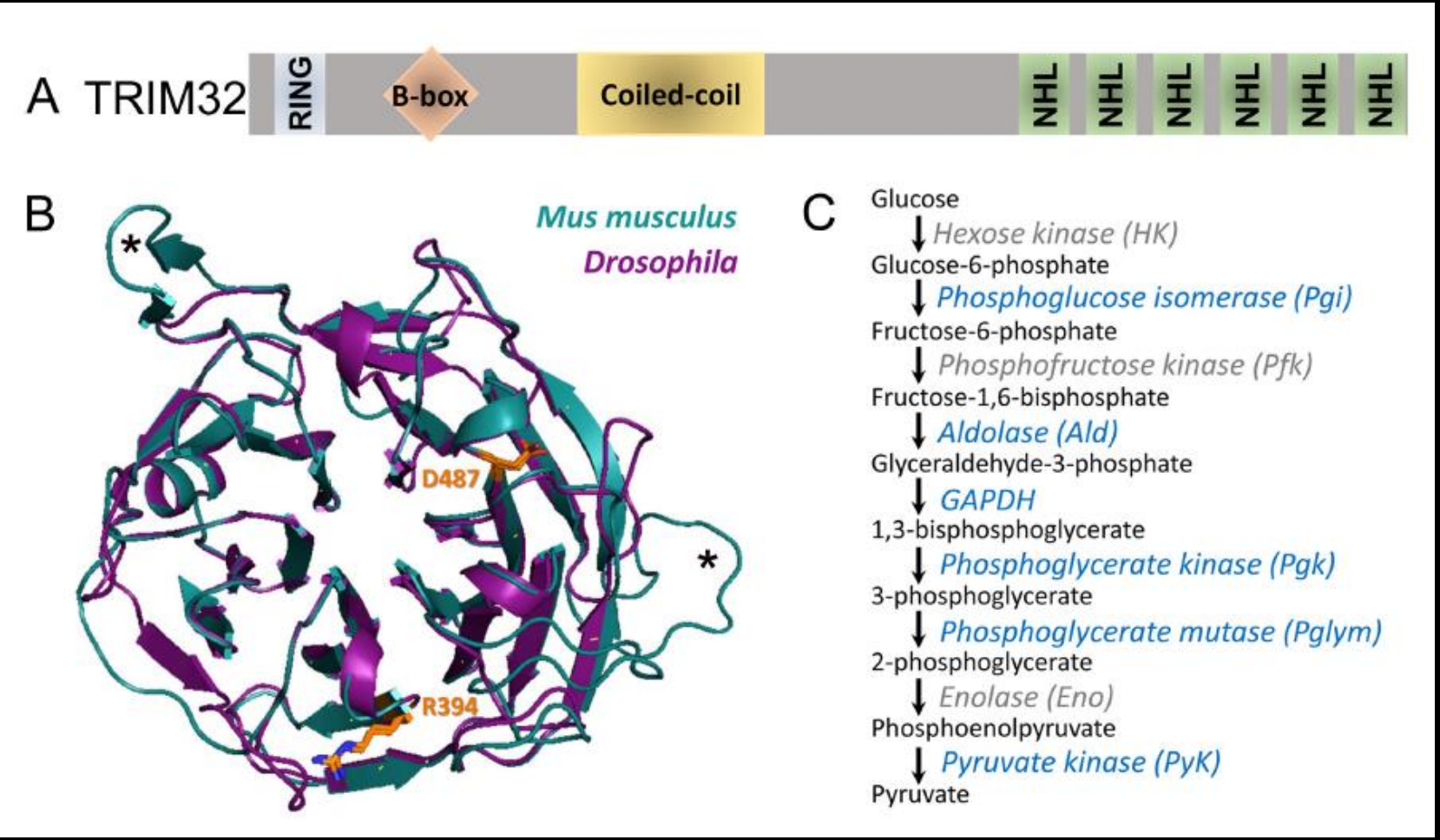

(A) Schematic showing the RING, B-box, coiled-coil, and NHL domains in TRIM32. (B) Superimposed protein structures of the six NHL repeats in *Drosophila* (magenta) and Mus musculus (blue) TRIM32. Each NHL repeat consists of four antiparallel beta sheets that are arranged toroidally around a central axis. Mouse NHL has two additional loops (asterisks) not present in the fly protein. The positions and orientation of both R394/R1114 and D487/D1211 are identical between Mus musculus and *Drosophila* (orange). (C) The glycolytic pathway. Peptides corresponding to enzymes that co-purified with TRIM32_NHL are shown in blue.

Figure 2. *Drosophila* TRIM32 physically interacts with the glycolytic enzymes Ald and Pglym78.

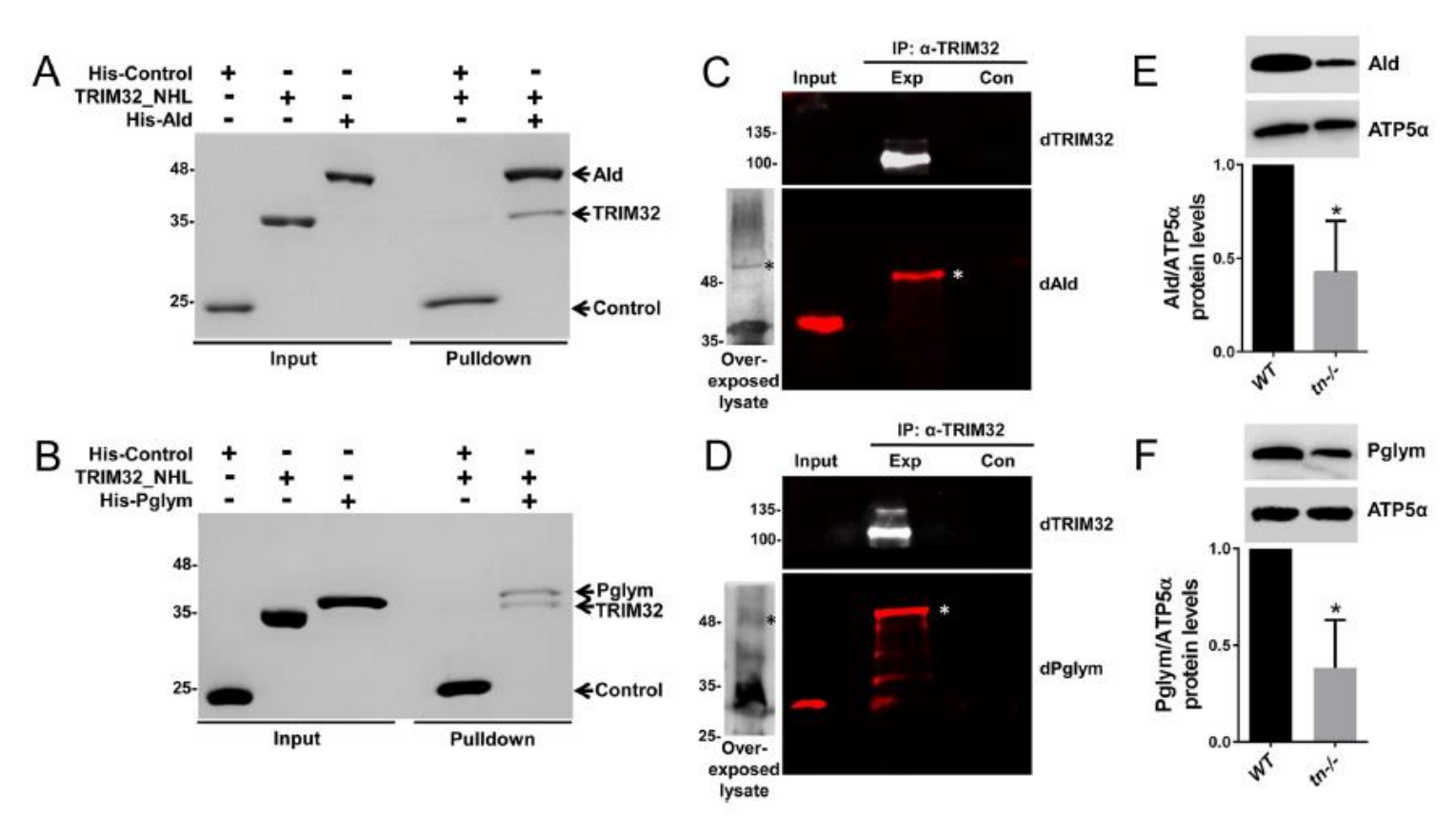

(A,B) In vitro binding assays. Untagged TRIM32_NHL was incubated with either the His-tagged SCIN control protein or the His-tagged candidate proteins Ald (A) or Pglym (B). After washing in 300 mM NaCl and 0.1% Triton, each of these protein complexes was separated by SDS-PAGE followed by Coomassie staining. Ald and Pglym proteins directly bind the NHL region of TRIM32, while no interaction with the His-SCIN control protein is observed. (C,D) Western blotting with antibodies against *Drosophila* Ald (dAld; C) or *Drosophila* Pglym (dPglym; D) detects higher molecular weight bands (asterisk) upon immunoprecipitation of *Drosophila* TRIM32, but not in control lanes. The observed molecular weights of Ald or Pglym in input larval lysates (~30 mg) is predominant over a higher migrating form that can be visualized after overexposure of blots with concentrated lysate (~300 mg). (E,F) Western blots showing that mutations in tn reduce Ald (E) or Pglym (F) protein levels ~ 50% quantitated relative to ATP5a in L3 larvae. N = 3. Mean +/- SD (*, $p<0.05$).

Figure 3. Loss of TRIM32 decreases glycolytic flux and reduces muscle tissue size.

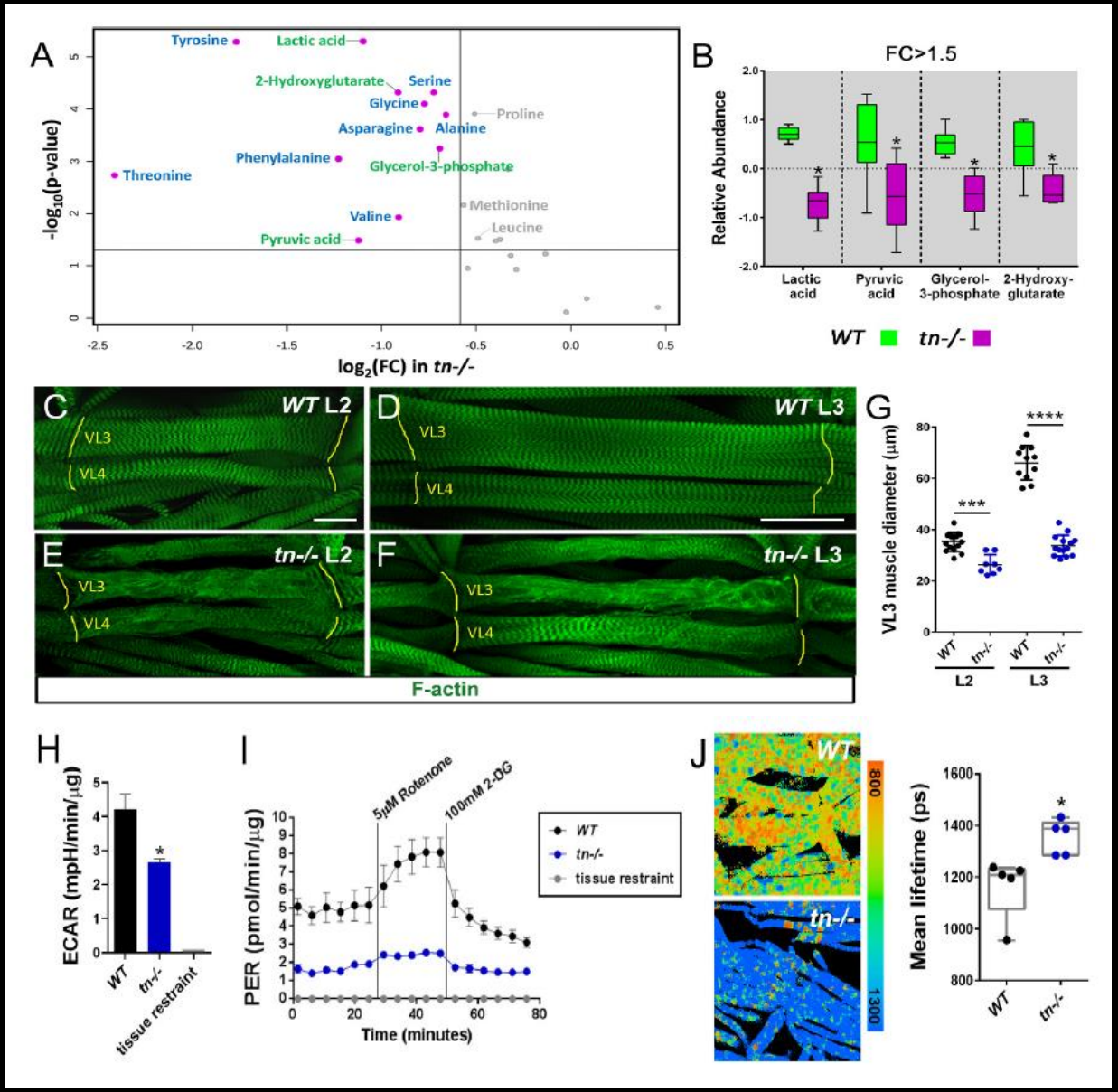

(A) Volcano plot illustrating fold change (FC) (log base 2) compared with p-value (- log base 10) between WT and *tn-/-* L3 larvae. Vertical line represents FC >1.5. Horizontal line depicts a significance level p<0.05. Metabolites that are reduced in tn-/- larvae include indicators of glycolytic flux (green) and amino acids (blue). Metabolites in gray are significant, but exhibit a FC <1.5. (B) Box and whisker plot of terminal glycolytic metabolites significantly reduced upon loss of TRIM32. N = 6. (C–F) Ventral longitudinal muscles 3 (VL3) and 4 (VL4) stained with phalloidin to visualize F-actin (green). (C,D) The stereotypical morphology of *WT* muscles is not altered as overall muscle size increases from the L2 (C) to the L3 (D) stage. (E,F) In addition to sarcomeric disorganization, the VL3 and VL4 muscles are noticeably smaller in *tn-/-* larvae during L2 (E) and L3 (F) development. Muscle attachment sites (MASs) are denoted by yellow lines. (G) Scatter plot depicting VL3 muscle diameter. The diameter of *WT* muscles increase from the L2 to the L3 stage. This cell size increase is abolished in *tn-/-*. N 8. (H) Bar graph shows that ECAR measurements are decreased in isolated *tn-/-* muscle carcasses compared to *WT.* N =4. (I) Analysis of the glycolytic rate in *WT* or *tn-/-* muscle tissue after subtraction of mitochondrial-produced acidification. This PER is diminished upon loss of TRIM32. N = 4. (J) NADH lifetime image comparison of *WT* and *tn-/-* muscles. Box and whisker plot shows *WT* muscles have significantly lower NADH lifetime, indicative of higher glycolytic flux, than *tn-/-*. N = 5. Mean +/- SD. (****, p<0.001; ***, p<0.01; *, p<0.05; n.s., not significant). Scale bars: 25 mm (C,E), 50 mm (D,F).

Figure 4. Muscle defects are cell autonomous and can be rescued upon stabilization of glycolytic enzyme levels.

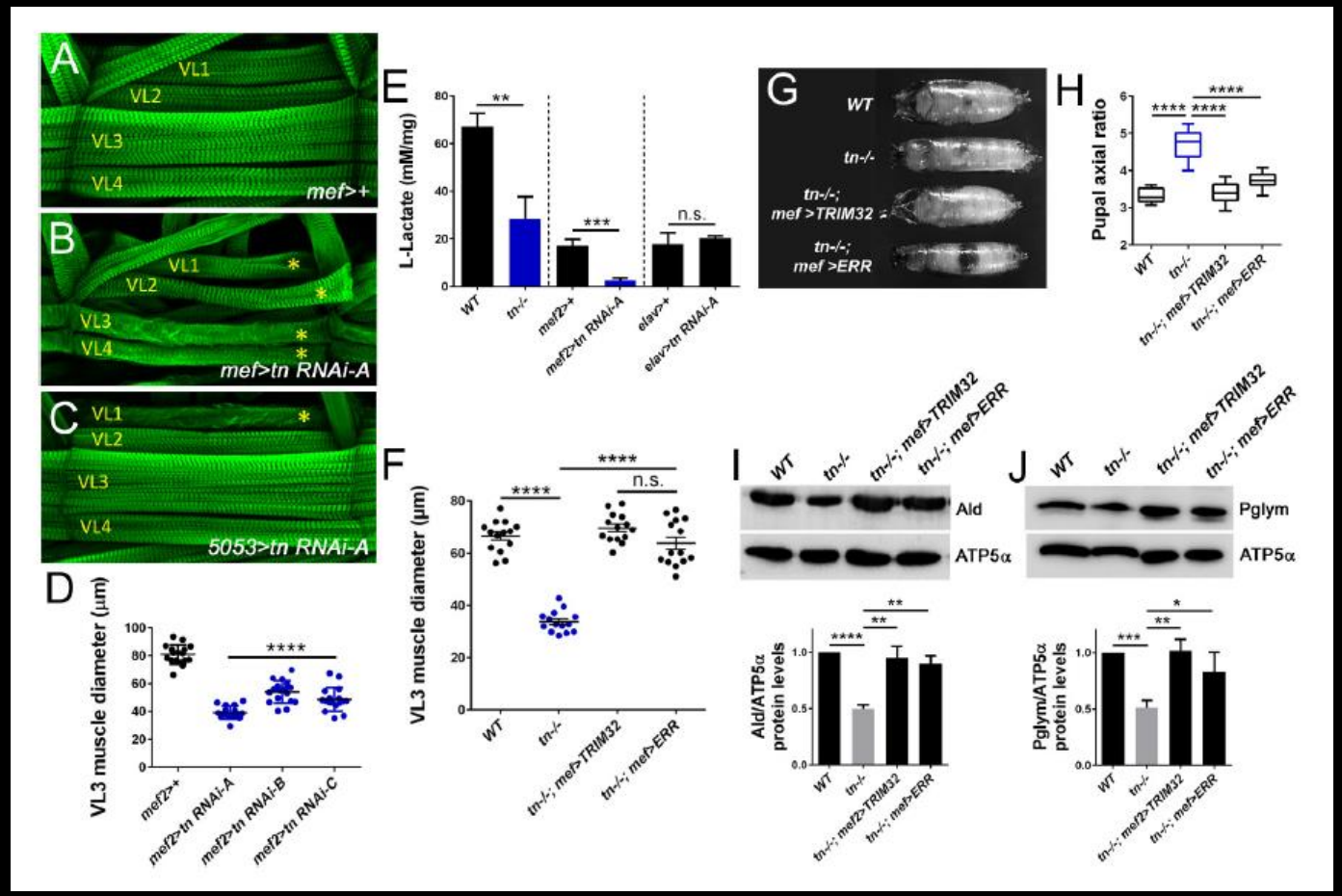

(A–E) Knockdown of TRIM32 in muscle tissue decreases muscle size and reduces lactate levels. (A–C) Phalloidin-labeled VL1-4 muscles in a representative hemisegment of the indicated genotypes. (A) mef2>+ control muscles appear *WT*. (B,C) RNAi knockdown of *tn* in all muscles with *mef2*-Gal4 (B) or only muscle VL1 using the 5053-Gal4 driver (C) show a reduction in muscle size (asterisk). (D) Knockdown of tn mRNA transcripts with three independent UAS-*tn RNAi* constructs in muscle tissue under control of the mef2 promoter (*mef2 >tn RNAi*) show reduced VL3 muscle diameter compared to *mef2/+* VL3 muscles. N 10. (E) Bar graph reveals a cell autonomous role for TRIM32 in muscle tissue. L-lactate levels in muscle carcasses are decreased upon loss of TRIM32 in all tissues. Induction of *tn* RNAi in muscle, but not neuronal tissue, reduces the concentration of muscle-derived lactate. N > 8. (F–J) Muscle-specific expression of TRIM32 (*tn-/-, mef >TRIM32*) or ERR (*tn-/-, mef >ERR*) in a *tn-/-* background attenuates the loss of muscle size, muscle contraction, and stabilizes glycolytic protein levels. (F) Scatter plot shows that the reduced VL3 muscle diameter upon loss of TRIM32 is restored upon expression of TRIM32 or ERR in muscle tissue. N 10. (G,H) The inability to contract body wall muscles in *tn-/-* causes elongated pupae. Muscle-specific expression of TRIM32 or ERR restores muscle contraction. (G) Representative pupal cases of the indicated genotypes. (H) Quantitation of pupal axial ratios represented by a box and whisker plot. N = 10. (I,J) Western blots showing the relative amounts of Ald or Pglym protein relative to the ATP5α loading control. Both Ald and Pglym protein levels are stabilized upon TRIM32 or ERR expression in muscle tissue compared to *tn-/-*. N = 3. Mean +/- SD (****, p<0.001; ***, p<0.01; **, p<0.05; *, p<0.01; n.s., not significant).

Figure 5. Amino acid supplementation is sufficient to improve *tn-/-* muscle mass.

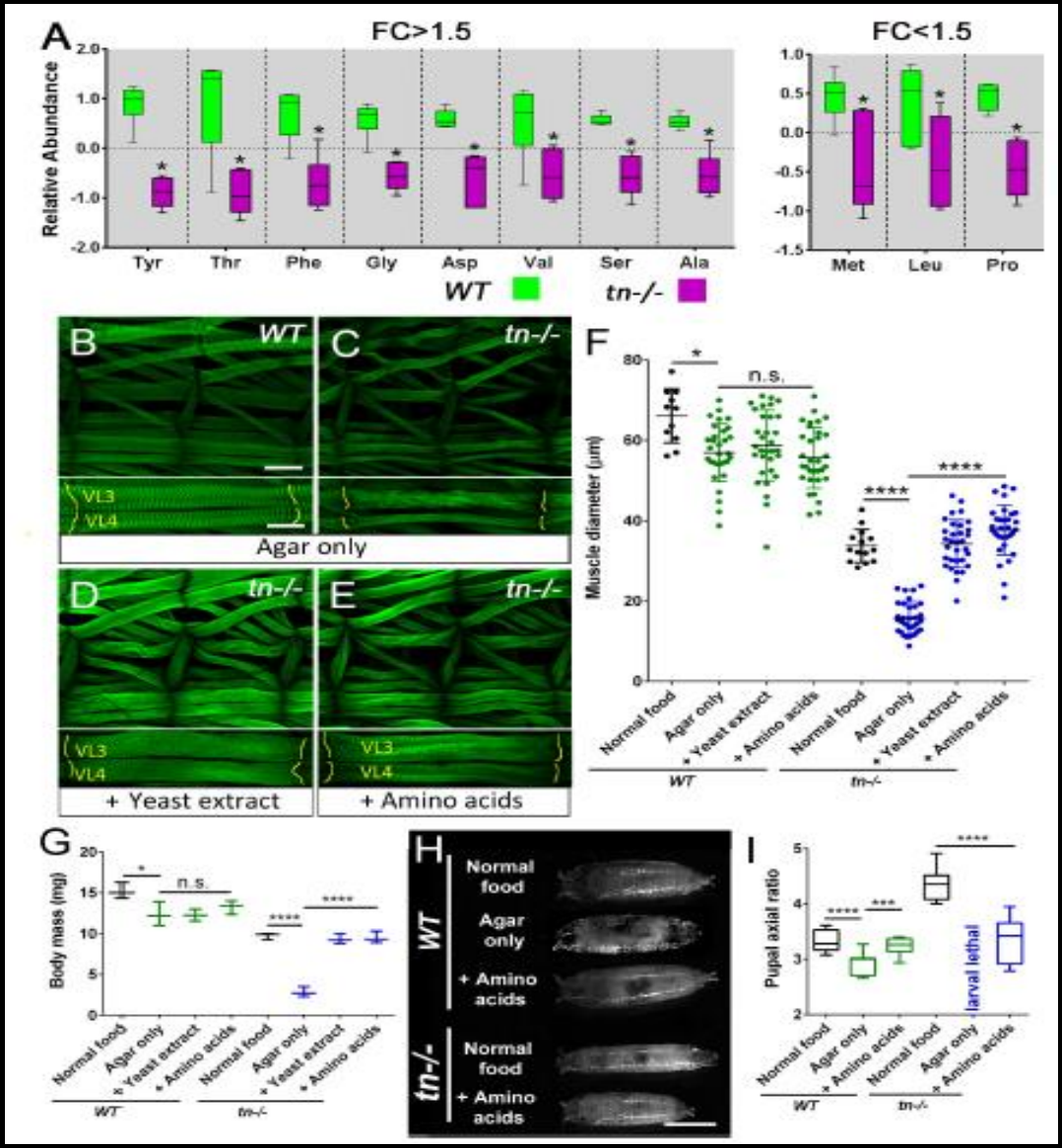

(A) Box and whisker plots showing the relative abundance of individual amino acids in L3 larvae with a FC >1.5 (left panel) or FC <1.5 (right panel) that are significantly reduced upon loss of TRIM32. N = 6. (B–E) Maximum intensity projections of *WT* (B) or *tn-/-* (C–E) L3 muscles stained for F-actin. Upper panel depicts two complete hemisegments and lower panel focuses on the VL3 and VL4 muscles. MASs are denoted by yellow lines. (B) An example of thinner *WT* musculature reared on agar as a sole nutritional source. (C) Muscles in larvae deficient for TRIM32 are substantially thinner when raised on agar alone. (D,E) Suppression of the reduced muscle diameter is observed in *tn-/-* muscles supplemented with total yeast extract (D) or amino acids (E) compared to *tn-/-* muscles alone. (F) Scatter plot showing the diameter of muscle VL3 in *WT* or *tn-/-* exposed to the indicated nutritional diets. N>32. (G) Average body mass measurements of *WT* or *tn-/-* L3 larvae. Ten individuals were weighed for each biological replicate that was performed in triplicate. (H) Representative pupal cases grown on the indicated diets. (I) The axial ratio (length/width) of pupal cases represented by box and whisker plots. N >10. Mean +/- SD. (****, $p<0.001$; *, $p<0.05$; n.s., not significant). Scale bars: 100 mm (A-D, upper panel), 50 mm (A-D, lower panel), 1 mm (H).

Figure 6. TRIM32 maintains glycolytic-mediated growth in the larval brain.

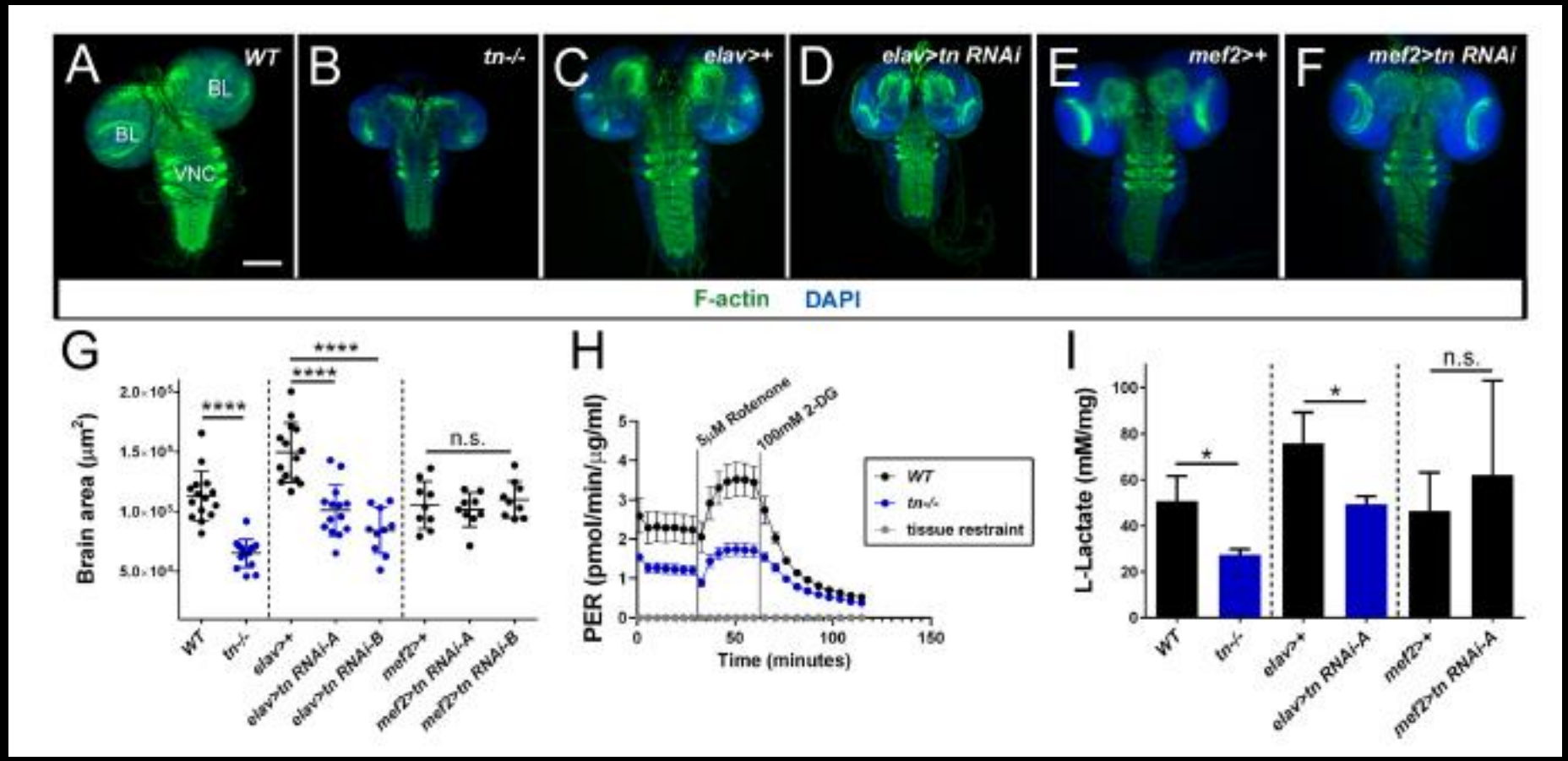

(A–F) L3 larval brains labeled with DAPI (blue) and F-actin (green). (A) A representative micrograph of a *WT* larval brain showing the individual brain lobes (BL) and the ventral nerve cord (VNC). (B) The overall size of *tn-/-* brains is reduced due to mutations in *tn*. (C) Control brains expressing the pan-neuronal *elav*-Gal4 driver. (D) RNAi knockdown of *tn* in neurons under control of the *elav* promoter causes smaller brains. (E,F) Expression of *mef2*-Gal4 alone (E) or *mef2 >tn RNAi* in muscle tissue does not alter brain size (F). (G) Scatter plot depicting the entire brain area (including the BL and VNC) of *WT*, *tn-/-*, Gal4 driver controls, or tissue-specific tn RNAi knockdown brains. N 9. (H) Glycolytic rate assay shows a reduction in the proton efflux rate (PER) upon loss of TRIM32 in isolated L3 larval brains. The glycolytic rate is calculated after subtraction of mitochondrial-produced acidification. N = 4. (I) Bar graph representing L-lactate levels in isolated larval brain tissue. Only loss of TRIM32 in brain, but not muscle tissue, caused a reduction in L-lactate levels. N 15. Scale bar: 100 mm (A–F). Mean +/- SD. (****, $p<0.001$; ***, $p<0.01$; n.s., not significant).

Figure 7. Loss of TRIM32 reduces Pvr-induced glycolytic tumor growth.

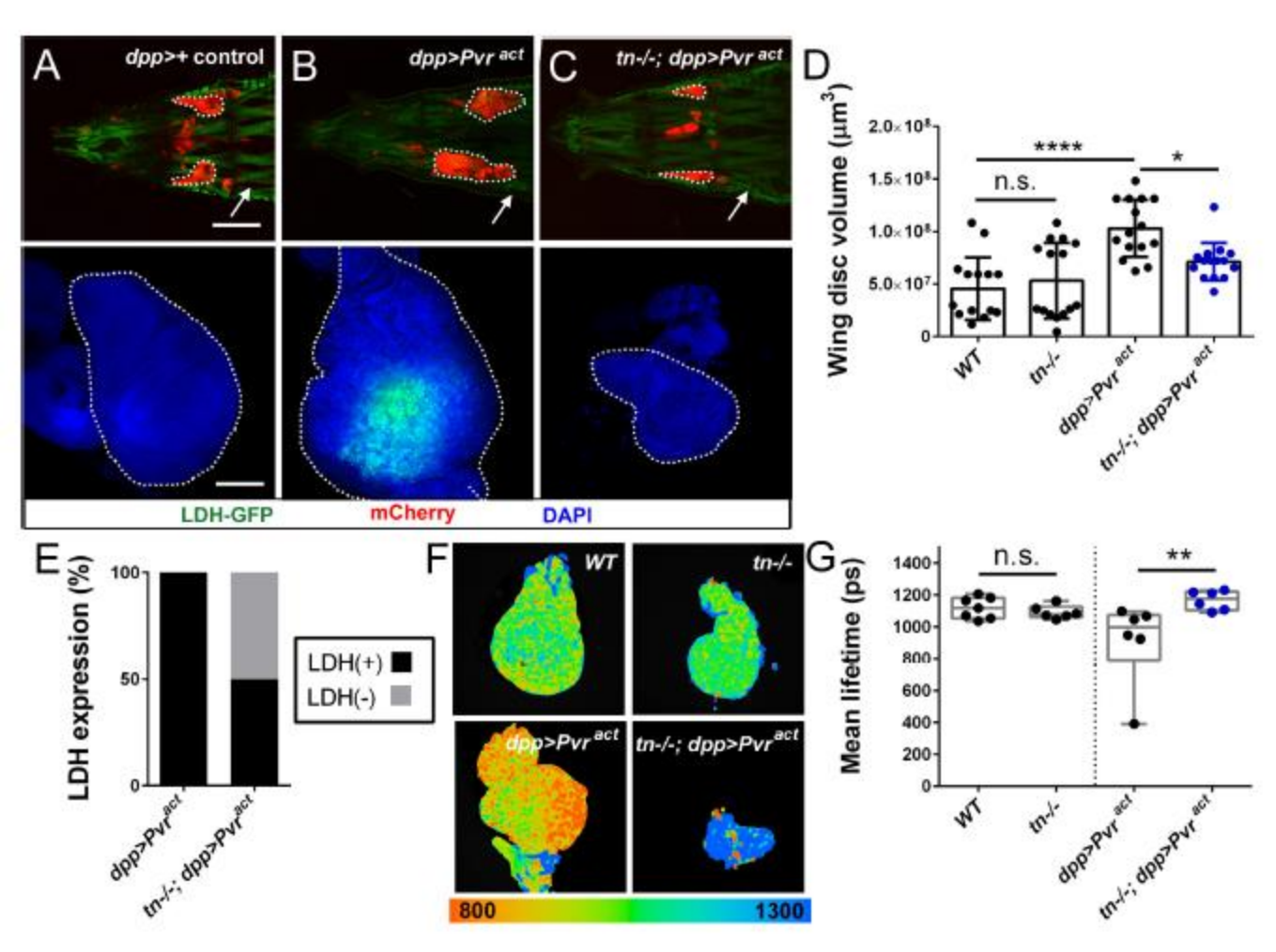

(A–C) Either intact (upper panel; red) or isolated (lower panel, blue) wing discs from L3 larvae of the indicated genotypes. LDH-GFP is high in somatic muscles (white arrow). Wing discs are outlined (white dotted outlines). (A) The normal size and shape of control *dpp-Gal4/+* wing discs. (B) Overexpression of the activated Pvr receptor (dpp >Pvract) causes tissue overgrowth and an increase in LDH-GFP expression (green). (C) Tumor growth in a *tn-/-* host is dramatically reduced in size. (D) Overall wing disc volumes are represented in this column plot. N 15. (E) Approximately 50% of LDH-GFP(+) cells induced by activated Pvr expression is reduced upon loss of TRIM32. N = 20. (F) Representative fluorescence lifetime micrographs of control (*WT* or *tn-/-*) or tumorous (*dpp >Pvr^{act}* or *tn-/-; dpp >Pvr^{act}*) wing discs.(G) Box and whisker plot confirms no difference in the glycolytic profile between *WT* or *tn-/-* discs. The decreased lifetime in *dpp >Pvr^{act}* discs, indicative of higher glycolytic flux, is reduced upon loss of TRIM32. N = 6. Mean +/- SD. (****, $p<0.001$; *, $p<0.05$; n.s., not significant). Scale bars: 0.5 mm (A-C, upper panels), 100 mm (A-C, lower panels).

Figure 8. Model for TRIM32 function in the regulation of cell size.

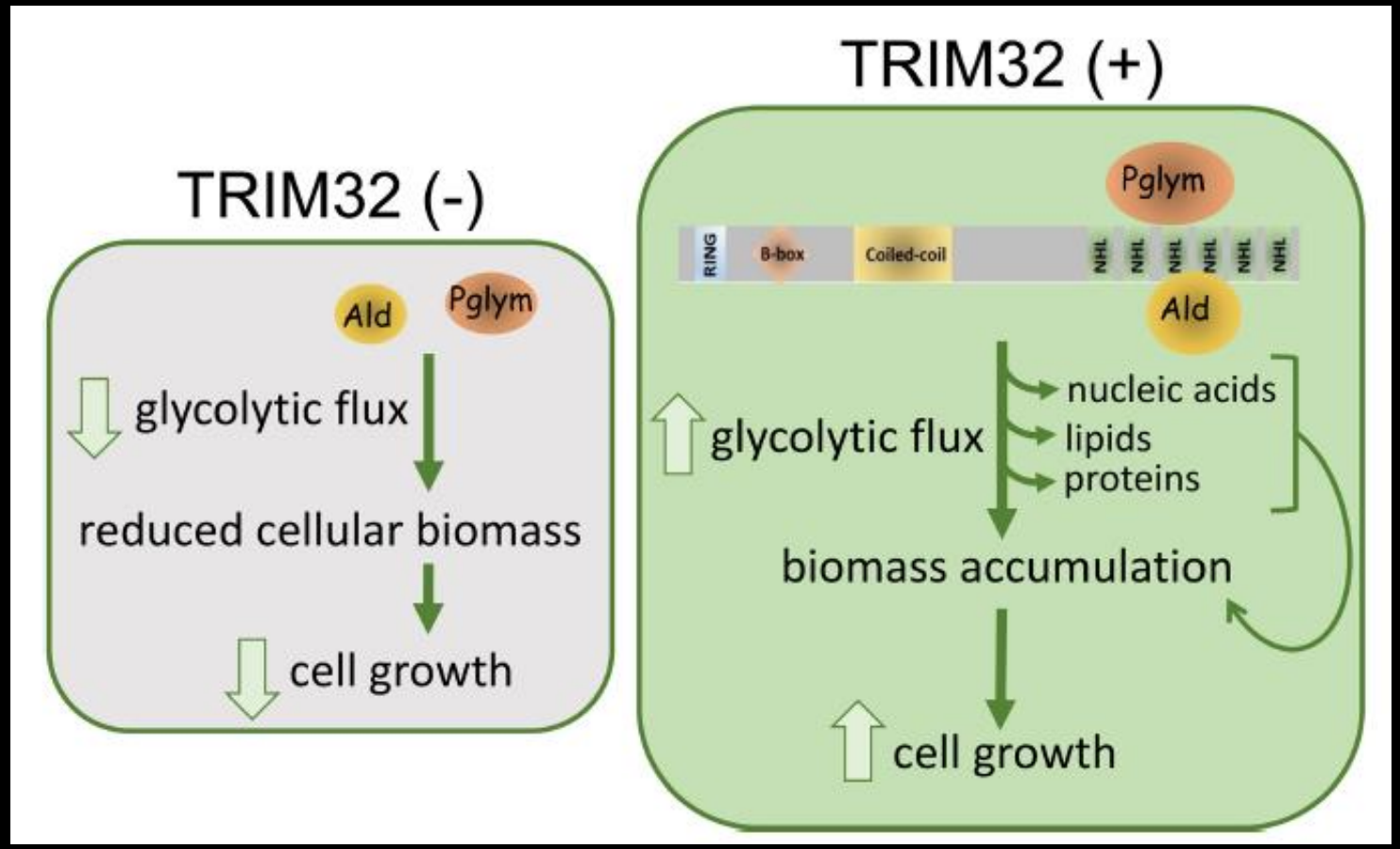

Biochemical interactions between TRIM32 and glycolytic enzymes such as Ald or Pglym cooperate in maintaining glycolytic activity for the synthesis of macromolecules required for cell growth. Loss of TRIM32 results in reduced levels of glycolytic enzymes, reduced glycolytic pathway intermediates, and compromises cell growth.